Furosemide Cocrystals: Structures, Hydrogen Bonding and Implications for Properties

Bethany I. Harriss[a], Liana Vella-Zarb[a], Claire Wilson[b] and Ivana Radosavljevic Evans[a]*

[a]Department of Chemistry, Durham University, Science Site, Durham DH1 3LE, UK

[b]Diamond Light Source, Didcot, OX11 0DE, UK

*ivana.radosavljevic@durham.ac.uk

Abstract

In this paper we report the crystal growth of four cocrystals of furosemide (4-chloro-2-[(2-furanylmethyl)amino]-5-sulfamoylbenzoic acid), a loop diuretic drug used for the treatment of hypertension and oedemas, prepared with *p*-aminobenzoic acid, nicotinamide and isonicotinamide as coformers. We present four new crystal structures and elucidate the intermolecular interactions present in the cocrystals. The structures display interesting supramolecular chemistry: a number of different synthons, as well as short strong hydrogen bonds with partial proton transfer and indications of proton disorder. Using powder X-ray diffraction, solid state NMR and thermal analysis, we provide evidence for the preparation of bulk samples of two compositions, namely, the 1:1 cocrystal of furosemide and *p*-aminobenzoic acid and 2:1 cocrystal of furosemide and isonicotinamide, highlighting the general necessity of such multi-technique approaches to characterisation of organic solids (including cocrystals and

solvates) prepared by grinding methods. Finally, we correlate the structural features reported for the first time in this work with the previously published pharmacologically relevant properties (solubility and intrinsic dissolution rate) of the furosemide cocrystals.

1. Introduction

Aqueous solubility and intestinal permeability of the active pharmaceutical ingredient (API), together with the dissolution of the formulated product, are three major factors which determine drug absorption and ultimately its efficacy. The Biopharmaceutics Classification System (BCS) classifies drug substances into four groups according to their solubility and permeability properties: class I (high permeability, high solubility), class II (high permeability, low solubility), class III (low permeability, high solubility) and class IV (low permeability, low solubility).[1] Overcoming the low permeability problem is primarily a task for formulation scientists, and much work has been targeting the development of permeability-enhancing excipients.[2] Improving the solubility of solid drug substances, on the other hand, is an important and topical research goal in the area of organic solid state chemistry, and cocrystallisation is emerging as an increasingly prominent approach to achieving this goal.

Cocrystals can be broadly described as crystalline multi-component adducts comprising neutral molecules held together by noncovalent interactions. In pharmaceutical cocrystals, the key components are API molecules and appropriate benign coformer molecules, typically substances on the GRAS list.[3] Design and preparation of cocrystals are widely thought of as based on the supramolecular synthon approach[4], *i. e.* on the existence of complementary functional groups in the API and coformer molecules. With compatible functional groups, noncovalent interactions (primarily hydrogen bonding) are likely to arise and lead to cocrystal formation.

Furosemide (FS, Figure 1), 4-chloro-2-[(2-furanylmethyl)amino]-5-sulfamoylbenzoic acid, is a loop diuretic drug used for the treatment of hypertension and oedemas arising from cardiac, renal and hepatic failure.[5] It is a class IV drug according to the BCS, suffering from both low permeability and low solubility.[6] The furosemide permeability and delivery-related issues have been addressed by a number of approaches, the most recent ones being emulsification and the use of mesoporous materials as carriers.[7-9] Cocrystallisation is amongst methods with the potential to provide a significant improvement in solubility, according to the recent findings of Goud *et al.*[10] The formation of cocrystals between furosemide and eight different coformers (caffeine, urea, *p*-aminobenzoic acid, acetamide, nicotinamide, isonicotinamide, adenine and cytosine) was reported and the improved solubility and dissolution of these materials relative to pure furosemide was demonstrated. However, only two of the compositions (caffeine and cytosine cocrystals) were obtained as single crystals which are needed for accurate structure determination by X-ray diffraction, for elucidation of the hydrogen bonding interactions leading to cocrystal formation and for structure-property correlations; in the remaining six cases, the cocrystal structures remained unknown.

A further problem arising from the absence of accurate crystal structures can be a limited ability to establish with a high degree of certainty the phase purity and identity of the bulk material characterised. Ueto *et al.*[11] have determined the crystal structures of four forms of the furosemide-nicotinamide cocrystals using laboratory powder X-ray diffraction. In this work, a large number of restraints were used in the Rietveld refinements of the non-hydrogen atoms (bond length and angle restraints, planar restraints on the phenyl, furan and pyridine rings, on carboxyl groups and on amide groups); all hydrogen atoms were placed geometrically and fixed

during the refinements. This again resulted in a lack of accurate and precise structural information needed to establish the key intermolecular interactions.

In this paper we report successful crystal growth of four furosemide cocrystals, prepared with *p*-aminobenzoic acid, nicotinamide and isonicotinamide as coformers. We present four new crystal structures and elucidate the intermolecular interactions present in these cocrystals. Using powder X-ray diffraction, solid state NMR and thermal analysis, we provide evidence for the preparation of bulk samples of two compositions, namely, the 1:1 cocrystals of furosemide and *p*-aminobenzoic acid and 2:1 cocrystals of furosemide and isonicotinamide, highlighting the general necessity of such multi-technique approaches to characterisation of organic solids (including cocrystals and solvates) prepared by grinding methods. Finally, we address the implications of the structural features found in this work for the previously published pharmacologically relevant properties of the furosemide cocrystals.

2. Experimental

2.1. **Materials:** Acetone was obtained from Fischer Chemicals (99.98 %). All other chemicals were obtained from Sigma Aldrich: furosemide ($\geq$ 98 %), nicotinamide ($\geq$ 99.5 %), isonicotinamide (99 %), *p*-aminobenzoic acid (99 %) and acetonitrile (99.5 %).

2.2. **Cocrystallisation:** Cocrystallisation of furosemide and *p*-aminobenzoic acid, nicotinamide and isonicotinamide coformers was attempted by solvent evaporation method from a variety of solvents and by neat and liquid-assisted grinding. We describe below only the preparations which gave the desired pure products.

FS – NCT (1:1): Equimolar quantities of FS (99 mg, 0.300 mmol) and NCT (12.2 mg, 0.300 mmol) were weighed out, combined and dissolved in 1.5 ml of ethanol. The solution

was then refluxed for 10 minutes and left in a vial with pierced lid for the solvent to slowly evaporate at room temperature. Colourless elongated plate-shaped crystals started appearing after about 10 days.

FS – INA (1:1): Equimolar quantities of FS (33 mg, 0.100 mmol) and INA (12.2 mg, 0.100 mmol) were weighed out and dissolved separately in 1.0 ml of acetone and water, respectively. The solutions were then combined and left in a vial with pierced lid for the solvent to slowly evaporate at room temperature. Colourless elongated plate-shaped crystals started appearing after about 9 days.

FS – INA (2:1): Single crystals of FS-INA 2:1 grew in the same cocrystallisation batch described above, from equimolar quantities of FS (33 mg, 0.100 mmol) and INA (12.2 mg, 0.100 mmol). They were also elongated colourless plates, and could not be visually distinguished from the 1:1 cocrystals. FS – INA 2:1 bulk cocrystal material was prepared by weighing out stoichiometric quantities of FS (264 mg, 0.800 mmol) and INA (48.8 mg, 0.400 mmol) and grinding them in a mortar and pestle for 30 minutes after the addition of 1 mL of acetone. A further 1 mL of acetone was added after 5 minutes of grinding and an additional 0.5 mL after 10 and 20 minutes.

FS – PABA (1:1): Equimolar quantities of FS (99 mg, 0.300 mmol) and PABA (41.1 mg, 0.300 mmol) were weighed out, combined and dissolved in 1.5 ml of ethanol. The solution was then refluxed for 10 minutes and left in a vial with pierced lid for the solvent to slowly evaporate at room temperature. Colourless elongated plate-shaped crystals started appearing after about 1 day. The same cocrystal was obtained from an identical synthesis using 1.5 mL of methanol as solvent, with colourless elongated plate-shaped crystals

appearing after about 1 day. FS – PABA bulk cocrystal material was prepared by weighing out stoichiometric quantities of FS (264 mg, 0.800 mmol) and PABA (5109.6 mg, 0.800 mmol) and grinding them in a mortar and pestle for 30 minutes after the addition of 1 mL of acetone. A further 1 mL of acetone was added after 5 minutes of grinding and an additional 0.5 mL after 10 and 20 minutes.

2.3. **Single crystal X-ray diffraction:** Single crystal X-ray diffraction data on FS-NCT, FS-INA and FS-INA 2:1 were collected on a Bruker SMART 6000 diffractometer with a CCD area detector, using graphite monochromated MoK$_\alpha$ radiation. In each data collection, a full sphere of data was collected by a series of ω scans, using a frame width of 0.3 ° in ω and exposure times between 20 and 40 seconds per frame, depending on the crystal. The raw data were collected using the SMART software and integrated using the SAINT suite of programs; [12] this included performing an empirical absorption correction in SADABS and reduction in XPREP. Single crystal X-ray diffraction data on FS-PABA cocrystals were collected on beamline I19 at Diamond Light Source, using a wavelength of 0.6889 Å and a standard hemisphere data collection (sample to detector distance 60 mm, 2θ detector position 30°). Data were collected as 1sec/° exposures, with 0.5mm Al beam attenuation. Structure solution was carried out using SIR92 and structure refinement on F^2 was carried out using CRYSTALS.[13, 14] Positional and anisotropic atomic displacement parameters (adps) were refined for all non-hydrogen atoms. A mixed hydrogen atom treatment was used: most hydrogen atoms were placed geometrically treated using a riding model, except for those involved in hydrogen bonding, whose fractional coordinates and isotropic atomic displacement parameters were freely refined. All crystallographic details are given in Table 1.

2.4. **Powder X-ray diffraction:** Powder X-ray diffraction data were collected on a Bruker D8 ADVANCE diffractometer ($CuK_{\alpha1,2}$ radiation) and a LynxEye detector. Patterns were recorded in ranges between 2 and 60° using a step size of 0.014 °. Data analysis was carried out using Topas-Academic software.[15]

2.5. **Solid state NMR:** Solid state C^{13} NMR spectra were recorded on a Varian VNMRS 400 spectrometer. CP-MAS measurements were carried out using a 6.8 kHz spinning rate and a contact time of 1.0 ms. Spectra were referenced to neat tetramethylsilane.

2.6. **Thermal analysis:** DSC measurements were carried out using TA DSC Q1000 instrument equipped with a nitrogen purge gas. 4-5 mg of sample was typically used for analysis. The heating rate was 10°/min.

Table 1: Crystallographic details for furosemide cocrystals.

	FS-NCT 1:1	FS-INA 1:1	FS-INA 2:1	FS-PABA 1:1
Empirical formula	$C_{18}H_{17}ClN_4O_6S$	$C_{18}H_{17}ClN_4O_6S$	$C_{30}H_{28}Cl_2N_6O_{11}S_2$	$C_{19}H_{18}ClN_3O_7S$
Molar mass/ g mol^{-1}	452.87	452.87	783.61	467.88
Temperature/ K	120(2)	120(2)	120(2)	100(2)
Crystal system	Monoclinic	Monoclinic	Monoclinic	Monoclinic
Space group	$P2_1/n$	$P2_1/n$	$P2_1/n$	$P2_1/n$
a/ Å	4.8206(3)	12.8613(15)	5.0178(11)	26.823(5)
b/ Å	20.6135(14)	5.3305(6)	38.527(8)	4.7607(10)
c/ Å	19.1406(12)	29.105(3)	17.031(4)	18.427(4)
β/ deg	93.291(2)	100.016(2)	94.353(3)	122.37(3)
Volume/ Å^3	1898.9(2)	1965.0(4)	3283.0(12)	1987.3(10)
Z	4	4	4	4
Reflections collected	19263	15181	24650	17604
Observed reflections	3336	3448	5701	4461
Parameters	291	291	471	304
Goodness of fit	0.93	0.92	0.92	0.99
R indices (I/σ=2)	R = 0.0445	R = 0.0374	R = 0.0978	R = 0.0402
	$R_w = 0.0776$	$R_w = 0.0731$	$R_w = 0.1296$	$R_w = 0.0917$
R indices (I/σ=0)	R = 0.0747	R = 0.0553	R = 0.1307	R = 0.0592
	$R_w = 0.0908$	$R_w = 0.0814$	$R_w = 0.1370$	$R_w = 0.1274$

3. Results and discussion

The furosemide molecule possesses a considerable potential for intermolecular interactions with coformer molecules *via* three functional groups which can give rise to hydrogen bonding (the sulfonamide group SO_2NH_2, the carboxyl group COOH and the NH group); these are complemented by the coformer molecules chosen (Fig. 1). The variety of hydrogen bonding interactions found in the cocrystals characterised in this work are depicted in Fig. 2 and discussed for each individual cocrystal separately.
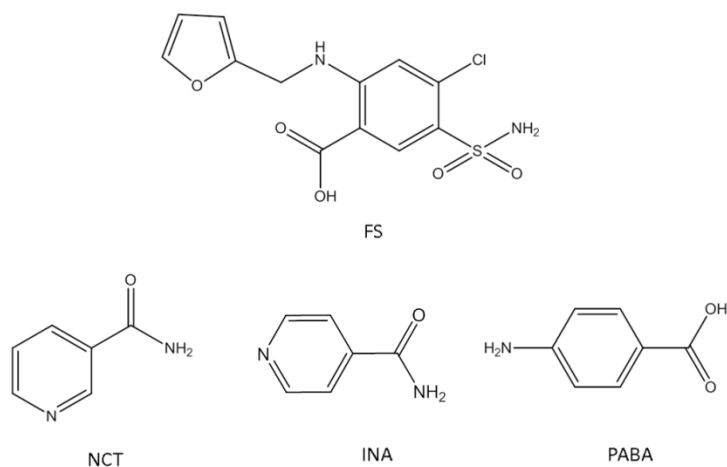
Figure 1: Molecular structure schemes for furosemide (FS), *p*-aminobenzoic acid (PABA), nicotinamide (NCT) and isonicotinamide (INA).
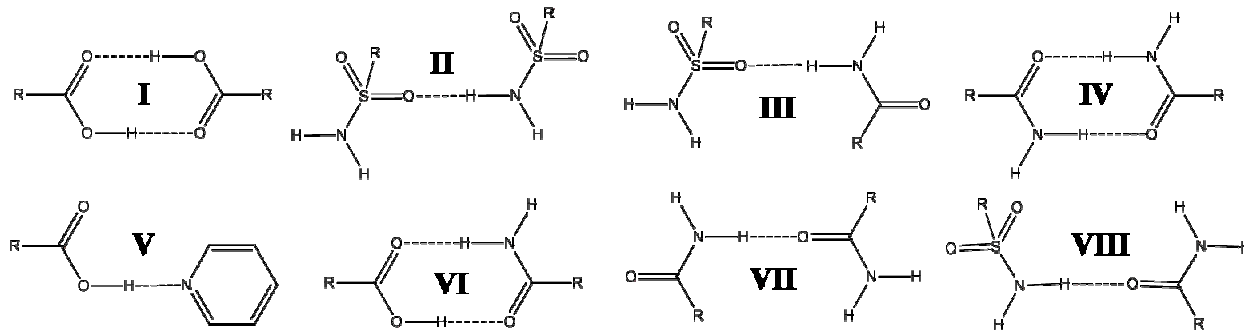
Figure 2: Hydrogen bonding synthons in furosemide cocrystals reported in this work (*vide infra*).

3.1. **FS-NCT 1:1 cocrystal**

FS-NCT 1:1 crystal structure: The single crystals obtained from an equimolar mixture of FS and NCT in ethanol by slow solvent evaporation correspond to the thermodynamically stable polymorph I identified previously by PXRD,[11] crystallising in the monoclinic space group $P2_1/n$ with unit cell parameters a = 4.8206(3) Å, b = 20.6135(14) Å, c = 19.1406(12) Å, β = 93.291(2)°. The asymmetric unit contains one FS molecule and one NCT molecule (Fig. 3). The shortest hydrogen bonding interaction occurs between pairs of FS and NCT molecules through synthon **V** (O(20)-H(201)···N(27)), $d_{D...A}$ = 2.556(4) Å, Fig. 3 and Fig. 4a), which then loosely connect *via* synthon **III** (N(24)-H(241) ···O(16)) into zig-zag chains running parallel to the *b*-axis, Fig. 4a. Perpendicular to this direction, the chains stack with FS molecules interacting through synthon **II** (N(18)-H(182)···O(17), $d_{D...A}$ = 2.902(5) Å) and NCT molecules stacking *via* synthon **VII** (N(24)-H(242)···O(16), $d_{D...A}$ = 2.982(5) Å), Fig. 4b.

Table 2: Intermolecular hydrogen bonding distances and angles for the FS-NCT 1:1 cocrystal.

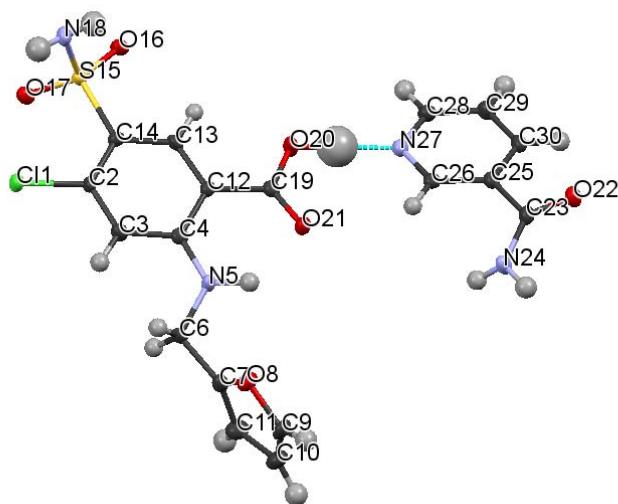| Interaction		D-H (Å)	H···A (Å)	D···A (Å)	∠ H-bond (°)
V	O(20)-H(201)···N(27)	1.08(6)	1.48(6)	2.556(4)	177(6)
II	N(18)-H(182)···O(17)	0.85(4)	2.16(4)	2.902(5)	147(4)
VII	N(24)-H(242)···O(16)	0.82(4)	2.20(4)	2.982(5)	155(3)
III	N(24)-H(241)···O(16)	0.89(4)	2.23(4)	3.062(5)	155(3)

Figure 3: The asymmetric unit in the FS-NCT form I with atom numbering. ADPs are drawn at the 50% probability level. Hydrogen atom labels omitted for clarity.
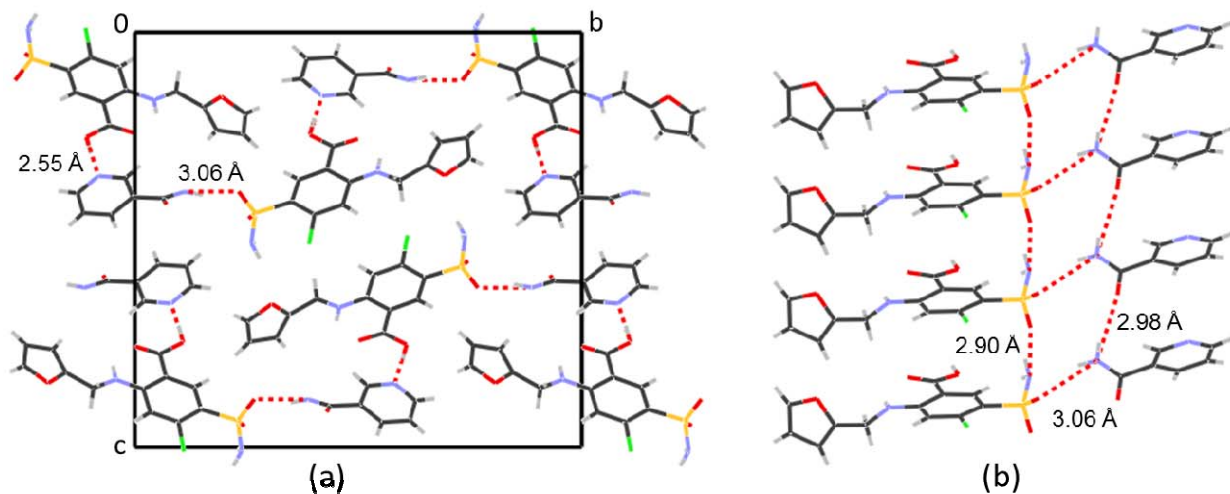

Figure 4: Diagram showing the hydrogen bonding present in the FS-NCT form I cocrystal. a) FS-NCT corrugated chains sustained by synthons **V** and **III**, viewed in the (*bc*) plane; b) hydrogen bonding in the perpendicular direction sustained by synthons **II** and **VII**. Numbers shown represent the D···A distances.

The hydrogen bonding parameters derived from our single crystal work shed new insight into intermolecular interactions in this cocrystal, which wasn't attainable from the heavily restrained powder diffraction based refinement.[11] The most notable and interesting new feature that our analysis reveals concerns the interaction in synthon **V**. This is an O-H···N hydrogen bond with a D···A distance of 2.55 Å and a D-H···A angle close to 180°, which classifies it as a short strong hydrogen bond (SSHB).[16] Typically of SSHBs, the O(20)-H(201)···N(27) interaction has an elongated O-H bonded distance of 1.08(6) Å and the isotropic temperature factor of H(201) is significantly larger than those of other hydrogen atoms in the structure. The O-H···N hydrogen bond with a D···A distance of 2.55 Å falls within the range of very short hydrogen bonds in which interesting proton behaviour and dynamics have been observed; examples include the temperature-induced reversible proton migration in 4-methylpyridine pentachlorophenol ($d_{O \cdots N}$ = 2.52 Å at 150 K)[17] and in 3,5-pyridinedicarbolylic acid and its deuterated analogue ($d_{O \cdots N}$ = 2.52 Å and 2.54 Å at 150 K).[18] For this reason, the FS-NCT cocrystals appear to merit further study by variable temperature single crystal neutron diffraction if sufficiently large crystals can be grown.

3.2. **FS-INA 1:1 cocrystal**

FS-INA 1:1 crystal structure: The formation of FS-INA 1:1 cocrystals by grinding was reported by Goud *et al.*;[10] however, single crystals were not obtained and no structural information was given. We successfully grew single crystals of this composition from an equimolar ratio of FS and INA by slow evaporation of a water – acetone solvent mixture. The FS-INA 1:1 cocrystals adopt monoclinic space group $P2_1/n$, with unit cell parameters a =

12.8613(15) Å, b = 5.3305(6) Å, c = 29.105(3) Å, β = 100.016(2)$^{\text{o}}$, and with one FS molecule

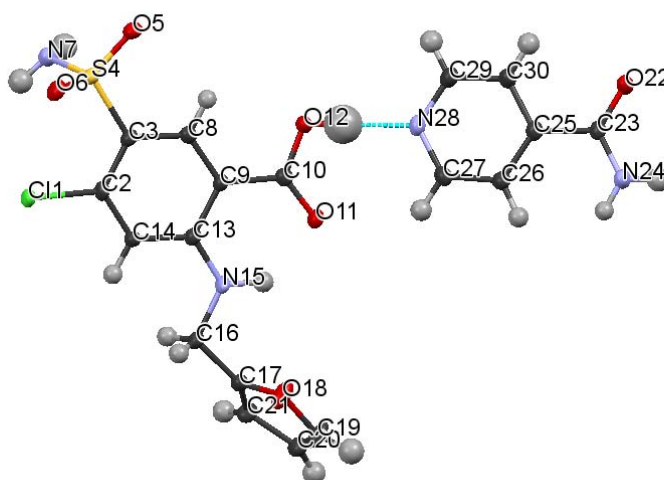and one INA molecule in the asymmetric unit (Fig. 5).

Figure 5: The asymmetric unit in the FS-INA 1:1 cocrystals with atom numbering. ADPs are drawn at the 50% probability level. Hydrogen atom labels omitted for clarity.

FS and INA molecules form pairs via synthon **V**, O(12)-H(121)···N(28), $d_{\text{D}\ldots\text{A}}$ = 2.64 Å, (Fig. 5 and Fig. 6). These pairs link up into centrosymmetric dimers sustained by synthon **IV**, N(24)-H(241)···O(22), $d_{\text{D}\ldots\text{A}}$ = 2.94 Å. Perpendicular to this, the INA dimers interact with FS molecules *via* synthon **VIII**, forming a moderate NHO hydrogen bond with $d_{\text{D}\ldots\text{A}}$ = 2.838(4) Å (Fig. 6 and Table 3). Finally, FS molecules interact *via* Cl(1)···O(5) weak halogen bonds, which, with Cl···O distances of 3.23 Å, appear to be at the boundary between bonding and non-bonding.[19]
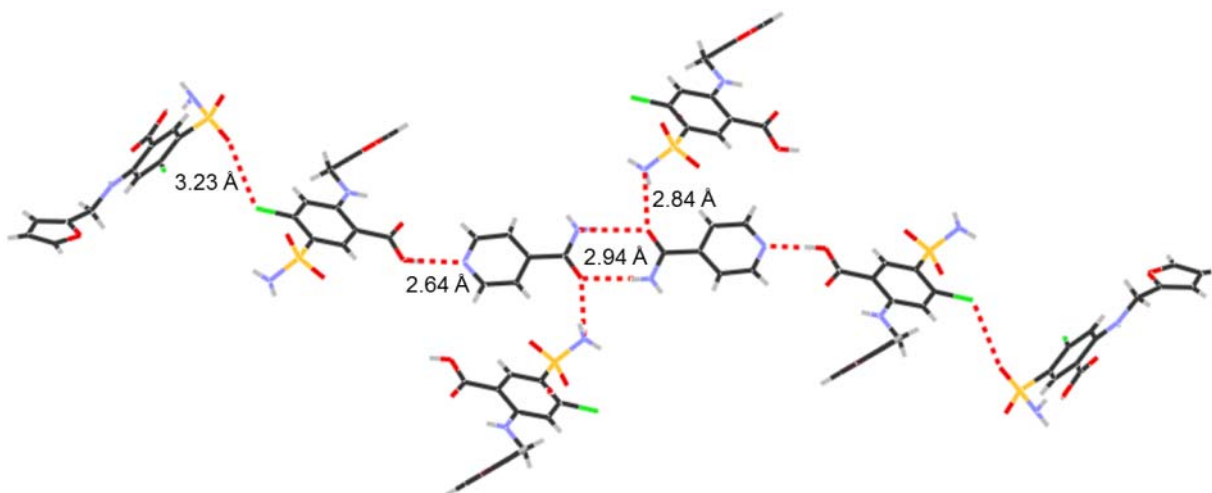
Figure 6: Intermolecular interactions present in the FS-INA 1:1cocrystal. Numbers shown represent the D···A distances.

Table 3: Intermolecular hydrogen bonding distances and angles for the FS-INA 1:1 cocrystal.

Interaction		D-H/ Å	H···A/ Å	D···A/ Å	∠ H-bond/ °
IV	N(24)-H(241)···O(22)	0.86(3)	2.08(3)	2.938(4)	172(3)
V	O(12)-H(121)···N(28)	0.91(5)	1.73(5)	2.638(4)	177(4)
VIII	N(7)-H(72)···O(22)	0.86(3)	2.03(3)	2.838(4)	156(3)

Our attempts to prepare bulk FS-INA 1:1 material by neat and wet grinding resulted in the formation of the 2:1 cocrystal (*vide infra*). For reference we give the calculated PXRD pattern obtained using the model derived from the single crystal X-ray structure analysis (Fig. 7).
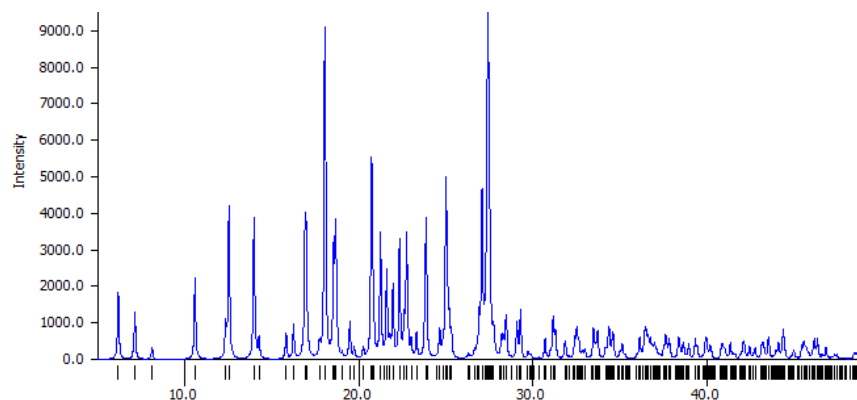
Figure 7: PXRD pattern (CuK$_{\alpha 1}$) for FS-INA 1:1 cocrystal calculated based on the structural model presented here.

3.3. **FS-INA 2:1 cocrystal**

FS-INA 2:1 crystal structure: Slow solvent evaporation from equimolar quantities of FS and INA from a water − acetone mixture also produced cocrystals in the 2:1 API-to-coformer ratio. FS-INA 2:1 crystallises with unit cell parameters a = 5.0178(11) Å, b = 38.527(8) Å, c = 17.031(4) Å, β = 94.353(3)$^{\rm o}$, in monoclinic space group $P2_1/n$, and with two FS molecules (referred to here as FS1 and FS2) and one INA molecule in the asymmetric unit. The most striking difference between the two crystallographically unique furosemide molecules is their conformation. Disregarding the sulphonamide group, FS1 is essentially planar, with the C(37)-N(39)-C(40)-C(41) torsion angle of 174$^{\rm o}$ (Fig. 8a-b); the corresponding torsion angle in FS2 is -83$^{\rm o}$, leading to a bent molecule (Fig. 8c-d). Similar bent conformations of the furosemide molecule are found in triclinic forms I and III of pure furosemide and also in the furosemide-caffeine cocrystals.[10, 20]

Both unique FS molecules in FS-INA 2:1 cocrystals contain disordered fragments: FS1 displays disorder in the sulphonamide group and FS2 displays disorder in the furan ring. In the FS1 molecule, the difference Fourier maps and the subsequent refinement revealed orientational disorder of the sulphonamide group, with two components whose occupancies refined to

14

0.51(1):0.49(1), approximately 30° apart. The FS2 molecule was best modelled with a 0.67(1):0.33(1) positional disorder of the furan ring. The true nature of the disorder of furosemide molecules in FS-INA 2:1 cocrystals, however, can only be probed by systematic variable temperature diffraction or solid state NMR study, which is outside the scope of this work.

Table 4: Intermolecular hydrogen bonding distances and angles for the FS-INA 2:1 cocrystal.

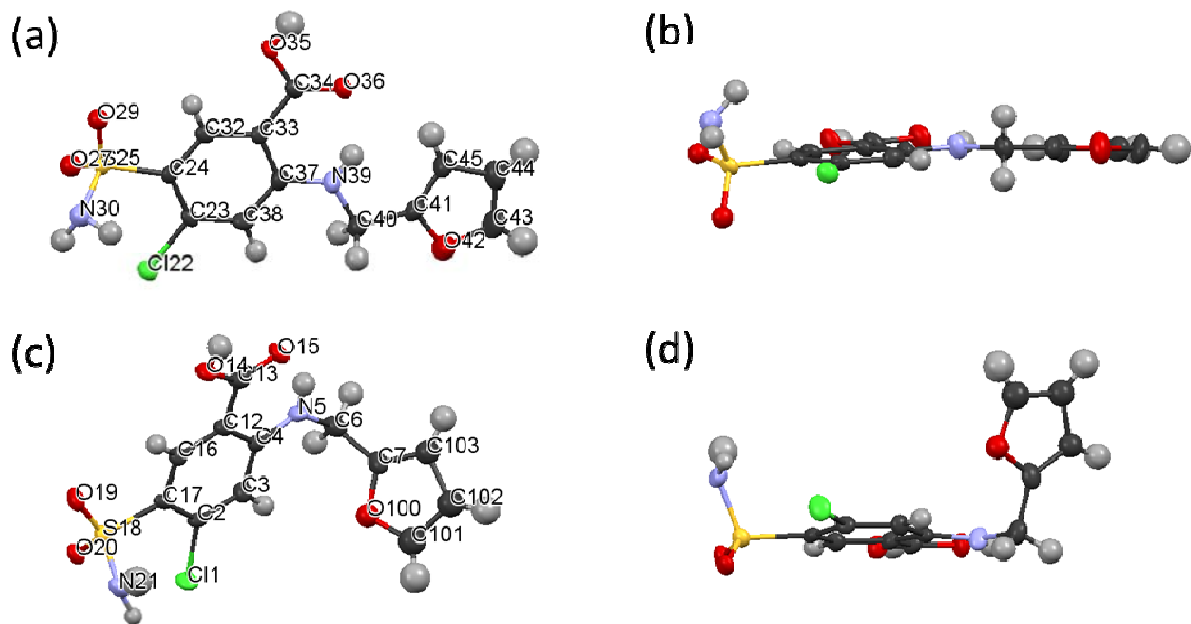| Interaction		D-H/ Å	H⋯A/ Å	D⋯A/ Å	∠ H-bond/ °
VI	O(14)-H(14)⋯O(46)	0.74(6)	1.88(7)	2.62(1)	176(7)
VI	N(48)-H(481)⋯O(15)	0.98(7)	1.88(7)	2.82(1)	160(6)
V	O(35)-H(35)⋯N(52)	0.93(7)	1.63(7)	2.55(1)	167(6)
III	N(48)-H(482)⋯O(20)	0.80(6)	2.27(7)	3.05(1)	166(5)

Figure 8: Two unique furosemide molecules in FS-INA 2:1 cocrystals. (a)-(b): two views of the FS1 molecule; (c)-(d): two views of the FS2 molecule. In each molecule, only one of the disordered fragments is shown for clarity. ADPs are drawn at the 50% probability level.

The INA molecule interacts with a FS1 molecule via synthon **VI**, with O(14)-H(14)···O(46) and N(48)-H(481)···O(15) donor-acceptor distances of 2.62(1) and 2.82(1) Å, respectively. This INA molecule also interacts strongly with a FS2 molecule through synthon **V** forming a short hydrogen bond, O(35)-H(35)···N(52) with $d_{O···N}$ = 2.55(1) Å, and weakly with another FS1 molecule through synthon **III**, N(48)-H(482)···O(20) with $d_{O···N}$ = 3.05(1) Å (Fig. 9). FS2 molecules also interact with like molecules through pairs of sulphonamide groups. These interactions are difficult to describe precisely due to the positional disorder present in these groups; there are two possible interactions arising from the two disordered components, which are presumably similarly favourable. Hydrogen bonding geometries are summarised in Table 4.
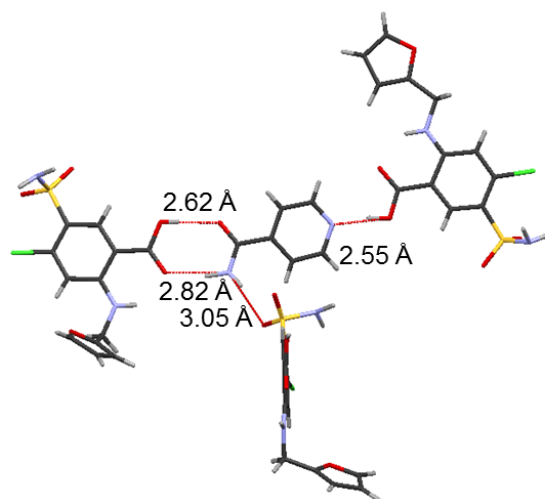

Figure 9: Intermolecular interactions present in the FS-INA 2:1 cocrystal. Numbers shown represent the D···A distances.

FS-INA 2:1 bulk material characterisation: The grinding procedure described in the Experimental Section yielded a cream coloured powder. The structural model obtained from the single crystal X-ray analysis was used to perform Rietveld fitting of the observed PXRD pattern, which confirmed the product obtained is nearly a single crystalline phase; a small amount of an impurity is suggested by the weak peak at about 15.3° 2θ, which is not predicted by the FS-INA

2:1 crystal structure (Fig. 10). The identity of this impurity is unknown; however, it is not any of the starting materials or the 1:1 FS-INA cocrystal. Given the preparation conditions, the most likely explanation is the formation of a very small amount of an acetone solvate. The fact that a single melting endotherm is observed in the DSC trace of this sample (*vide infra*) confirms that it is an essentially single phase product, with any impurity at a very minor level.
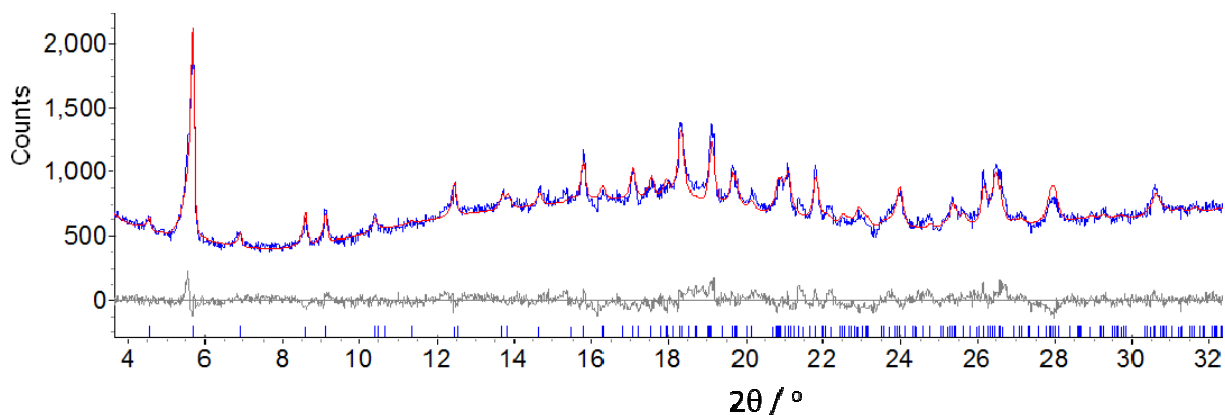

Figure 10: Rietveld fit for the FS-INA 2:1 cocrystal obtained by grinding. R_{wp} = 4.744%, a = 5.112(1) Å, b = 38.756(7) Å, c = 17.052(4) Å, β = 94.27(3) $^\circ$, V = 3369(1) Å^3.

Solid state ^{13}C NMR was performed on FS, INA, on the lightly mixed physical mixture of the two starting components and on the cocrystal product (Fig. 11a). The latter shows a number of chemical shift changes in the spectrum relative to pure FS and INA. In contrast, the spectrum of a 1:1 physical mixture of the reagents corresponds to the sum of the individual spectra of FS and PABA.
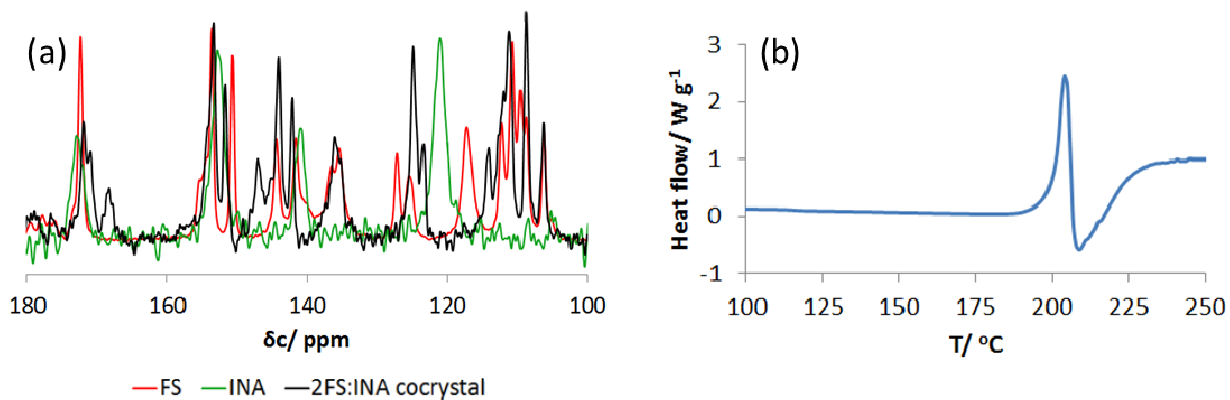
Figure 11: (a) Solid state ^{13}C NMR data showing an overlay of the FS, INA and the FS-INA 2:1 cocrystal spectra. (b) DSC (endothermic up) of FS-INA 2:1 cocrystal.

A DSC trace recorded on the FS-INA 2:1 cocrystal produced by grinding is depicted in Fig. 11b. This shows a single endotherm, corresponding to the melting temperature of 204.3^{o}C for the cocrystal. This melting point is between the measured melting points of the API and the coformer (220.7^{o}C and 158.0^{o}C, respectively), in agreement with a trend generally observed in cocrystals.[21]

The appearance of the PXRD pattern shown in Fig. 10 suggests that an amorphous component exists in the bulk product, which is not surprising in a product prepared by grinding of soft organic materials. This, however, necessitates additional characterisation by complementary techniques to rule out the possibility that the amorphous component represents an unwanted impurity. In this case, the NMR spectra and DSC curve together confirm that any amorphous component in the sample is the target cocrystal itself.

3.4. **FS-PABA 1:1 cocrystal**

FS-PABA 1:1 crystal structure: FS-PABA 1:1 cocrystals adopt monoclinic space group $P2_1/n$ with unit cell parameters a = 26.823(5) Å, b = 4.7607(10) Å, c = 18.427(4) Å, β = 122.37(3)$^{\circ}$, and with one FS molecule and one PABA molecule in the asymmetric unit (Fig. 11).
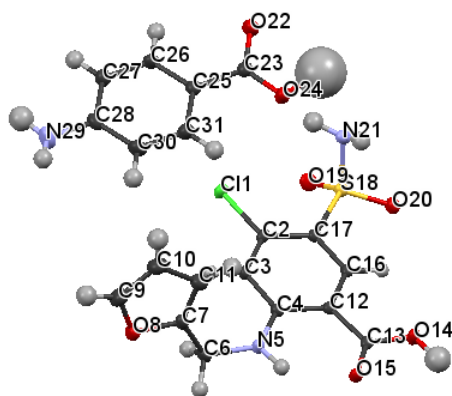

Figure 11: The asymmetric unit in the FS-PABA 1:1 cocrystals with atom numbering. ADPs are drawn at the 50% probability level. Hydrogen atom labels omitted for clarity.

Both types of molecules form dimers sustained by synthon **I**. Pairs of FS molecules form dimers through O(14)-H(141)···O(15) hydrogen bonding ($d_{O···O}$ = 2.613(4) Å), while PABA molecules pair via O(24)-H(241)···O(22) interactions ($d_{O···O}$ = 2.618(5) Å), Fig. 12a. Despite the same synthon and an essentially identical donor – acceptor distance in the two types of dimers, the hydrogen bonding in them differs significantly. In the FS dimers, the key hydrogen atom, H(141), is located on the O(4) donor ($d_{O(4)-H(141)}$ = 0.97(4) Å). The asymmetric nature of this hydrogen bond is manifested in the C-O atom distances in this COOH functional group; C(7)-O(3) and C(7)-O(4) bond length values of 1.237(3) Å and 1.319(3) Å clearly reflect the double and single character of these bonds, respectively.[18] By contrast, partial proton transfer occurs in the PABA dimer hydrogen bond. The O(24)-H(241) distance (1.21(9) Å) and a large isotropic

displacement parameter for H(241) suggest possible proton disorder in this hydrogen bonded dimer. In this case the distances $d_{C(23)-O(22)} = 1.278(3)$ Å and $d_{C(23)-O(24)} = 1.280(3)$ Å belong to the region between the C-O bond length distribution maxima representing single and double bonds;[18] this situation is consistent with a significant degree of proton transfer in the OHO hydrogen bond in the PABA dimer. PABA dimers are arranged in a herringbone motif (Fig. 12b), while the two types of dimers interact weakly via synthon **III**, N(29)-H(292)···O(20), forming an extended hydrogen bonding network. The O-H oxygen atom in PABA is also involved in a halogen bond with the chlorine atom of a FS molecule, C(2)-Cl(1)···O(24), with $d_{Cl···O} = 3.054(4)$ Å.
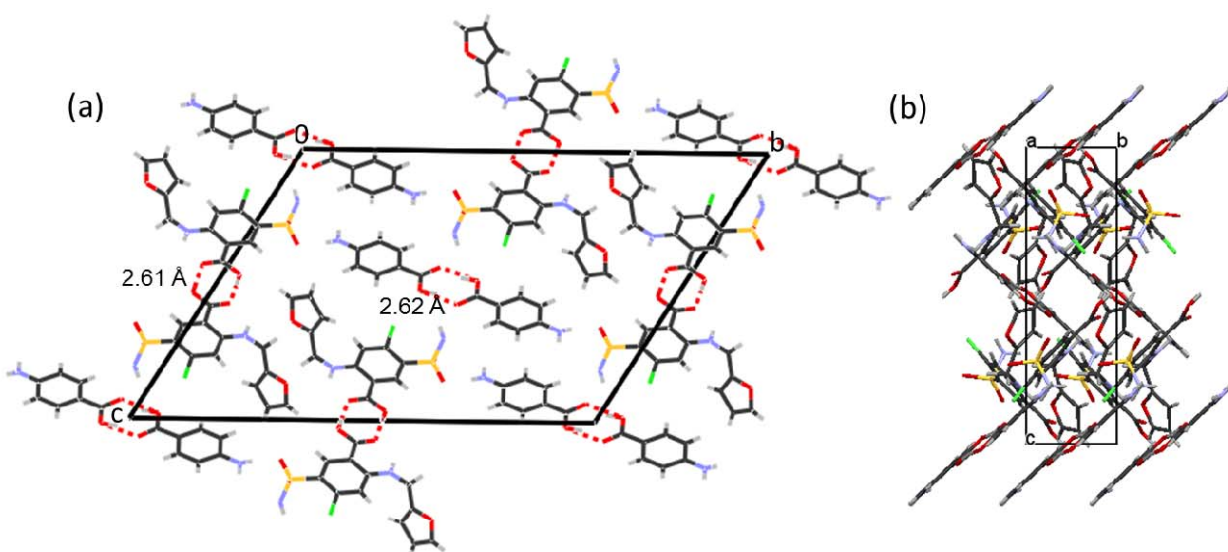

Figure 12: Intermolecular interactions in the FS-PABA cocrystal. a) FS and PABA dimers viewed in the (*bc*) plane; b) herringbone motif formed by PABA dimers, with interspersed FS dimers. Numbers shown represent the D···A distances.

20

Table 5: Intermolecular hydrogen bonding distances and angles for the FS-PABA cocrystal.

Interaction		D-H/ Å	H···A/ Å	D···A/ Å	∠ H-bond/ °
I	O(14)-H(141)···O(15)	0.97(4)	1.64(4)	2.613(4)	179(4)
I	O(24)-H(241)···O(22)	1.21(9)	1.45(9)	2.618(5)	160(9)
III	N(29)-H(292)···O(20)	0.86(4)	2.20(4)	3.054(4)	168(3)

FS-PABA bulk material characterisation: The liquid-assisted grinding procedure yielded an off-white (pale pink) powder. The structural model obtained from the single crystal X-ray analysis was used to perform Rietveld fitting of the observed PXRD pattern, which confirmed the product obtained is single phase (Fig. 13).
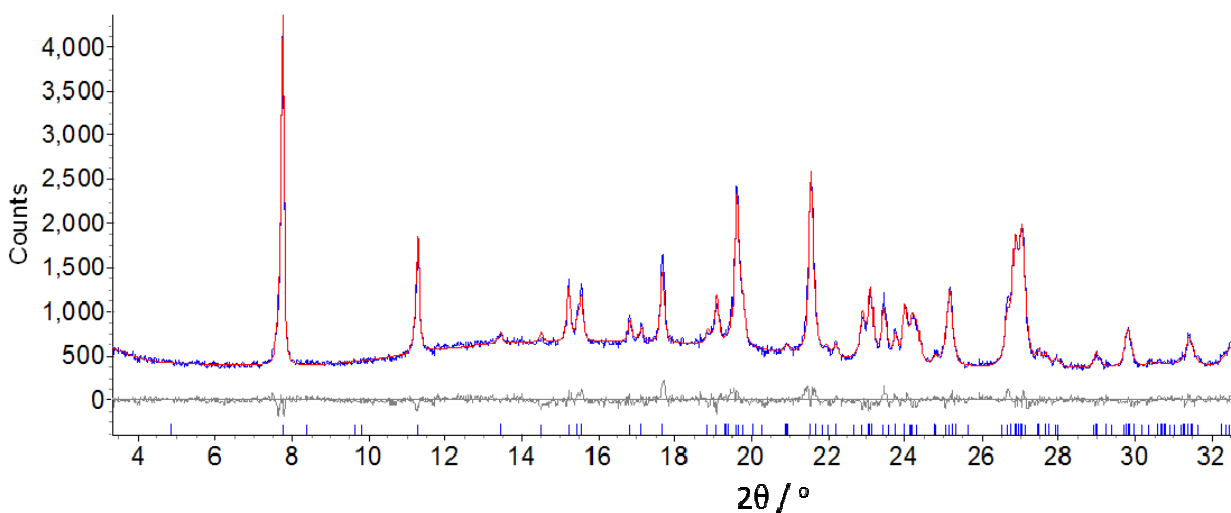

Figure 13: Rietveld fit for the FS-PABA cocrystal obtained by liquid-assisted grinding. R_{wp} = 4.955%, a = 27.004(2) Å, b = 4.8085(3) Å, c = 18.587(1) Å, β = 122.506(5) °, V = 2035.4(3) Å^3.
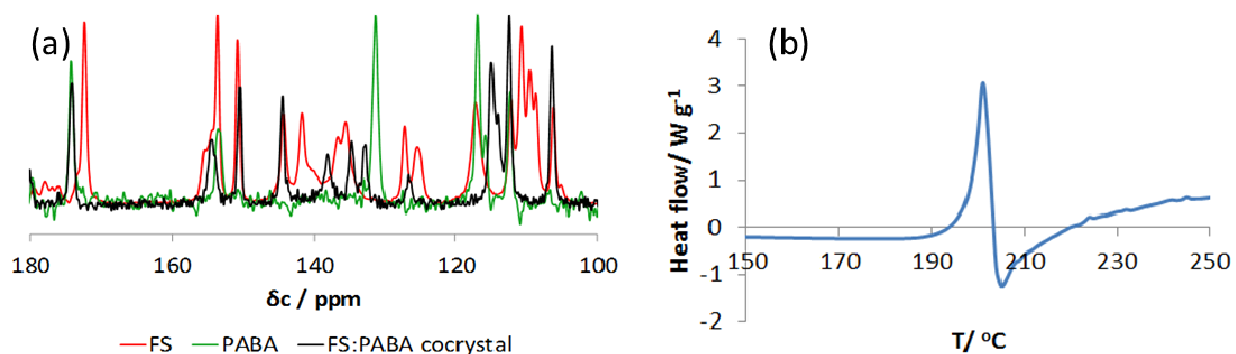
Figure 14: (a) Solid state ^{13}C NMR data showing an overlay of the FS, PABA and the FS-PABA cocrystal spectra. (b) DSC (endothermic up) of FS-PABA.

Solid state ^{13}C NMR was performed on the cocrystal, both individual components and on the physical mixture. Comparison reveals changes in the chemical shift of a number of peaks in the cocrystal spectrum with respect to pure FS and PABA. Finally, the DSC (Fig. 14b) confirms the obtained product to be a pure, single phase FS-PABA cocrystal through the presence of only one melting endotherm. The melting temperature for the cocrystal, 201.0 ^{o}C, is between the melting points of the API and the coformer (220.7 ^{o}C and 189.4 ^{o}C, respectively). These complementary techniques again demonstrate that a small amorphous component present in the product is not an impurity, but the target cocrystal.

4. Structure-property relationships

Goud et al.[10] have reported two sets of pharmacologically relevant properties, namely solubility and intrinsic dissolution rate in 10% ethanol – water, for pure FS and a number of its cocrystal compositions. The crystal structures of only two cocrystals (furosemide with caffeine, FS-CAFF and with cytosine, FS-CYT) were known at the time, which limited the scope for

rationalisation of the properties observed. Goud *et al.*[10] attributed a significant (almost 11-fold) increase in aqueous solubility of FS-CYT relative to pure furosemide to the fact that this composition forms a salt, *i.e.* the proton from the COOH group of FS is transferred to the basic ring N atom of the cytosine molecule. Secondly, they proposed that the stability of FS-CAFF, FS-CYT and FS-ADEN in 10% ethanol – water slurry was a consequence of these being congruently dissolving systems, made up of components of similar solubility. However, they found FS-PABA cocrystal to be an exception from this trend, being unstable and converting to furosemide within 24 hours, and also displaying the smallest improvement in solubility and intrinsic dissolution rate relative to pure FS.

The details of crystal structures and hydrogen bonding presented on our work can shed light on these observations. Firstly, none of the four compositions whose structures have been determined form salts, and this correlates well with their reported aqueous solubility values being lower than that of FS-CYT, although they are still higher than that of pure furosemide. Secondly, the FS-PABA structure is unique among the furosemide cocrystals in that the intermolecular interactions are stronger between pairs of molecules of the same component than between the API and the coformer molecules. As shown in Table 5, FS molecules form dimers through O-H···O hydrogen bonding with donor-acceptor distances of 2.613(4) Å, and these dimers then connect to PABA molecules *via* weak N-H···O interactions (donor-acceptor distances of 3.054(4) Å). These hydrogen bonding arrangements are very similar to those in pure furosemide, in which FS molecules also connect into carboxylic acid dimers (with donor-acceptor distances of 2.635(5) Å and 2.672(5) Å), which then weakly interact with other FS molecules *via* N-H···O interactions with donor-acceptor distances of 2.999(5) Å. These similarities in intermolecular interactions in

the pure FS and FS-PABA structures can account for an only modest increase of solubility and intrinsic dissolution rate of this cocrystal relative to pure API.

The FS-INA 1:1 cocrystal exhibits superior properties relative to pure furosemide: an increase of the solubility in 10 % EtOH-water at 24 h by a factor of 7.2 and an increase in the intrinsic dissolution rate in 10 % EtOH-water by a factor of 2.3. The issue with the FS-INA 1:1 cocrystal, however, is the low stability; the samples converted to furosemide within 24 hours in a 10 % EtOH-water slurry medium. The characterisation of the pharmacologically relevant properties of the FS-INA 2:1 cocrystal, reported here for the first time, is beyond the scope of this study. However, future work on this system includes measurements of solubility, intrinsic dissolution rate and stability using the same methodology employed by Goud *et al.* [10], in order to acquire data for meaningful comparisons.

5. Conclusions

Several different synthons are present in the forms of FS analysed in this work, as summarised in Table 6. However, some general trends can be observed. Synthons **II**, **III** and **V** are formed in most of the cocrystals containing the relevant functional groups. Comparisons of bond lengths and angles suggest that all occurrences of **II** and **III** are of moderate strength; however, in two out of three occurrences, synthon **V** displays very short D···A distances ($d_{N \cdots O} = 2.55$ Å) between the best hydrogen bonding donor and the best hydrogen bonding acceptor in each case, implying strong hydrogen bonding interactions.

Table 6: Synthons formed in the furosemide cocrystal structures determined in this work.

	I	II	III	IV	V	VI	VII	VIII
FS form 1	✓	✓						
FS-NCT 1:1		✓	✓		✓		✓	
FS-PABA 1:1	✓	✓	✓					
FS-INA 1:1				✓	✓			✓
FS-INA 2:1			✓		✓	✓		

In contrast, PABA molecules interact by SSHBs through synthon **I** to form dimers in the FS-PABA cocrystal. Whilst synthon **I** can form between FS molecules, it has been shown to be of only moderate strength in both pure FS and the FS-PABA cocrystal. The lack of alternative interactions for the FS COOH moiety in the FS-PABA cocrystal allows for formation of this synthon; however, in the presence of aromatic nitrogen moieties, this synthon does not compete favourably with synthon **V**. Previous studies have found carboxylic acid dimers to be favoured in the absence of competing interactions, whilst synthon **V** is dominant (77% of instances) when the relevant functionalities were present.[22] This correlates well with the results presented here.

AUTHOR INFORMATION

Corresponding Author

*ivana.radosavljevic@durham.ac.uk

REFERENCES

(1)   BCS
http://www.fda.gov/AboutFDA/CentersOffices/OfficeofMedicalProductsandTobacco/CDER/uc
m128219.htm
(2)   Thanki, K.; Gangwal, R. P.; Sangamwar, A. T.; Jain, S., *Journal of Controlled Release.*
2013, 170, 1, 15.
(3)   GRAS
http://www.fda.gov/Food/FoodIngredientsPackaging/GenerallyRecognizedasSafeGRAS/default.
htm
(4)   Desiraju, G. R., *Angewandte Chemie-International Edition in English.* **1995,** 34, 21,
2311.
(5)   Granero, G. E.; Longhi, M. R.; Mora, M. J.; Junginger, H. E.; Midha, K. K.; Shah, V. P.;
Stavchansky, S.; Dressman, J. B.; Barends, D. M., *Journal of Pharmaceutical Sciences.* **2010,**
99, 6, 2544.
(6)   Lindenberg, M.; Kopp, S.; Dressman, J. B., *European Journal of Pharmaceutics and
Biopharmaceutics.* **2004,** 58, 2, 265.
(7)   Ambrogi, V.; Perioli, L.; Pagano, C.; Latterini, L.; Marmottini, F.; Ricci, M.; Rossi, C.,
Microporous and Mesoporous Materials. **2012,** 147, 1, 343.
(8)   Ambrogi, V.; Perioli, L.; Pagano, C.; Marmottini, F.; Ricci, M.; Sagnella, A.; Rossi, C.,
European Journal of Pharmaceutical Sciences. **2012,** 46, 1-2, 43.
(9)   Zvonar, A.; Berginc, K.; Kristl, A.; Gasperlin, M., *International Journal of
Pharmaceutics.* **2010,** 388, 1-2, 151.
(10)   Goud, N. R.; Gangavaram, S.; Suresh, K.; Pal, S.; Manjunatha, S. G.; Nambiar, S.;
Nangia, A., *Journal of Pharmaceutical Sciences.* **2012,** 101, 2, 664.
(11)   Ueto, T.; Takata, N.; Muroyama, N.; Nedu, A.; Sasaki, A.; Tanida, S.; Terada, K.,
Crystal Growth & Design. **2012,** 12, 1, 485.
(12)   Bruker *SAINT Plus*, 6.22; Madison, Wisconsin.
(13)   Altomare, A. C., G.; Giacovazzo, A.; Guagliardi, A.; Burla, M.C.; Polidori, G.; Camalli,
M, *Journal of Applied Crystallography.* **1994,** 27, 437.
(14)   Betteridge, P. W.; Carruthers, J. R.; Cooper, R. I.; Prout, K.; Watkin, D. J., *Journal of
Applied Crystallography.* **2003,** 36, 1487.
(15)   Coelho, A. A.; Evans, J. S. O.; Evans, I. R.; Kern, A.; Parsons, S., *Powder Diffraction.*
2011, 26, 4, S22.
(16)   Steiner, T., *Angewandte Chemie-International Edition.* **2002,** 41, 1, 48.
(17)   Steiner, T.; Majerz, I.; Wilson, C. C., *Angewandte Chemie-International Edition.* **2001,**
40, 14, 2651.
(18)   Ford, S. J., Delamore, O. J., Evans, J. S. O., McIntyre, G. J., Johnson, M. R., Evans, I. R.,
Chemistry - A European Journal. **2011,** 17.
(19)   Wilcken, R.; Zimmermann, M. O.; Lange, A.; Joerger, A. C.; Boeckler, F. M., *Journal of
Medicinal Chemistry.* **2012,** 56, 4, 1363.
(20)   Babu, N. J.; Cherukuvada, S.; Thakuria, R.; Nangia, A., *Crystal Growth & Design.* **2010,**
10, 4, 1979.
(21)   Schultheiss, N.; Newman, A., *Cryst. Growth Des.* **2009,** 9, 6, 2950.
(22)   Weyna, D. R.; Shattock, T.; Vishweshwar, P.; Zaworotko, M. J., *Cryst. Growth Des.*
2009, 9, 2, 1106.

TOC Graphic and synopsis

Four new crystal structures of pharmaceutical molecule furosemide with GRAS coformers are reported and correlated with the known pharmacologically relevant properties of these materials. Furosemide carboxylic acid oxygen donor – coformer aromatic nitrogen acceptor is the dominant synthon, leading to the key intermolecular interactions in the cocrystals studied.